# Kinetic Study of the Oxidation of γ-L-Glutaminyl-4-hydroxybenzene Catalyzed by Mushroom (*Agaricus bisporus*) Tyrosinase

Juan Carlos Espín,* Sylvie Jolivet, and Harry J. Wichers

Agrotechnological Research Institute (ATO-DLO), Bornsesteeg 59, P.O. Box 17, 6700 AA Wageningen, The Netherlands

Despite the importance of the substrate γ-L-glutaminyl-4-hydroxybenzene (GHB) in the melanin biosynthesis pathway in mushrooms *Agaricus bisporus*, the kinetics of its oxidation catalyzed by tyrosinase has never been properly characterized. For this purpose GHB and its corresponding *o*-diphenol (GDHB) were isolated and purified from *A. bisporus* mushrooms. The kinetic constants that characterize the action of tyrosinase on GHB and GDHB are $V_{max}^{GHB} = 2.10 \pm 0.10$ μM/min, $K_m^{GHB} = 0.30 \pm 0.03$ mM, $V_{max}^{GDHB} = 210.0 \pm 7.3$ μM/min, and $K_m^{GDHB} = 7.80 \pm 0.41$ mM. The oxygen kinetic constants for tyrosinase in the presence of these compounds are $V_{max}^{O_2(GHB)} = 3.20 \pm 0.21$ μM/min, $K_m^{O_2(GHB)} = 1.50 \pm 0.12$ μM, $V_{max}^{O_2(GDHB)} = 200.2 \pm 8.1$ μM/min, and $K_m^{O_2(GDHB)} = 100.2 \pm 8.2$ μM. These values were compared to those obtained for the pair L-tyrosine/L-DOPA. The kinetic and structural reaction mechanisms of tyrosinase were corroborated for these physiological phenolic compounds.

**Keywords:** *Agaricus; GHB; GDHB; kinetics; mechanism; mushroom; tyrosinase*

## INTRODUCTION

Tyrosinase or polyphenol oxidase (EC 1.14.18.1) is the main enzyme involved in the enzymatic browning of mushrooms and other crops. This browning is an undesirable reaction that is responsible for less attractive appearance and loss in nutritional quality. Tyrosinase catalyzes two different reactions: the hydroxylation of monophenols to *o*-diphenols (monophenolase activity) and the oxidation of *o*-diphenols to *o*-quinones (diphenolase activity), which, in turn, polymerize to brown, red, or black pigments (Prota, 1988; Sánchez-Ferrer et al., 1995; Jolivet et al., 1998).

In *Agaricus bisporus* the main substrates of tyrosinase are tyrosine and γ-L-glutaminyl-4-hydroxybenzene (GHB) and their oxidative products DOPA and γ-L-glutaminyl-3,4-dihydroxybenzene (GDHB), respectively. GHB and its derivatives are present only in the *Agaricus* genus leading to a specific type of melanins: the GHB-melanins (Pierce and Rast, 1995). GHB is synthesized in mycelium grown on compost medium; the anilide occurs also in specific tissues of the fruit bodies, such as the stipe base, the skin, and, in larger amounts, the gills, where it can reach 2.5% of the dry matter (Stüssi and Rast, 1981; Jolivet et al., 1995; Soulier et al., 1993). GHB is considered as a precursor of spore wall melanins (Rast et al., 1979, 1981; Stüssi and Rast, 1981; Oka et al., 1981) and it may play, therefore, a role in (photo)protection. It has been suggested that one of GHB's oxidative products could also be involved in spore dormancy by inhibition of both mitochondrial respiratory enzymes and protein synthesis (Graham et al., 1977; Vogel et al., 1975, 1979). However, its function in mushroom is not yet well understood.

The monophenolase activity of mushroom tyrosinase on GHB has been previously measured by using the release of tritium (Boekelheide et al., 1979) in long assays, but such kinetic assays have, however, never been corroborated with current knowledge regarding the reaction mechanism of tyrosinase. This has been due mainly to the difficulty of isolating and purifying this compound together with the lack of sensitive and reliable assay methods.

The aim of the current work is to kinetically study the oxidation of GHB catalyzed by mushroom tyrosinase. The kinetic constants, which characterize the action of mushroom tyrosinase on GHB, GDHB, L-tyrosine, and L-DOPA, are determined as well as the oxygen constants for tyrosinase in the presence of these compounds to compare the catalytic power of tyrosinase on the GHB/GDHB and L-tyrosine/L-DOPA pairs. Kinetic and structural reaction mechanisms of tyrosinase previously proposed are corroborated by combining both kinetic and NMR assays (Rodríguez-López et al., 1992a; Ros et al., 1994a; Espín et al., 1995a,b, 1996, 1997a−f, 1998a−d).

## MATERIALS AND METHODS

**Reagents.** L-DOPA, L-tyrosine, and 3-methyl-2-benzothiazolinone hydrazone (MBTH) were purchased from Sigma (St. Louis, MO). All other reagents were of analytical grade and supplied by Merck (Darmstadt, Germany). Stock solutions of phenolic compounds were prepared in 0.15 mM orthophosphoric acid as solvent to prevent autoxidation. Milli-Q system (Millipore Corp., Bedford, MA) ultrapure water was used throughout this research. To dissolve the MBTH−quinone adducts, 2% (v/v) *N*,*N*′-dimethylformamide (DMF) was added to the assay medium (Winder and Harris, 1991).

**Enzyme Source.** Mushroom (*A. bisporus*) tyrosinase (1200 units/mg) was purchased from Fluka. The commercial preparation of tyrosinase showed one major isoform with an isoelectric point of 4.3 determined by isoelectric focusing and a major band of $M_r$ of 43000 in SDS−PAGE electrophoresis (results not shown). This major isoform was purified by using an anion exchange column (DEAE-Sepharose Fast Flow, length = 75 cm, diameter = 5 cm; Pharmacia, Uppsala,

* Author to whom correspondence should be addressed (fax 31-317-475347; e-mail J.C.ESPIN@ato.dlo.nl).

10.1021/jf981155h CCC: $18.00 
Published on Web 08/07/1999

Sweden). The column was equilibrated with 20 mM Bis-Tris buffer (pH 6). A stepwise gradient of increasing sodium chloride (NaCl) concentrations was applied (3 mL/min). Fractions containing this isoform were pooled, dialyzed, and concentrated by using an ultrafiltration cell (Amicon, Beverly, MA). The concentrate was used as source of enzyme. Commercial tyrosinases can differ substantially in their isoform pattern and protein content, even among different lots. This could be one of the reasons why variable results are reported in the literature. Therefore, a further purification of these commercial preparations is strongly recommended (Kumar and Flurkey, 1991).

**Isolation and Purification of GHB and GDHB.** GHB and GDHB were extracted from gills of mushrooms harvested at stage 6 (Hammond and Nichols, 1976). Gills were immediately frozen in liquid nitrogen and lyophilized. The $\gamma$-glutaminyl derivatives were extracted from 5 g of ground gill powder with 100 mL of 0.5% (w/v) sodium *m*-bisulfite in 1% (v/v) acetic acid. After centrifugation for 15 min at 5000*g*, the supernatant was collected and the pellet was submitted to a second extraction with 50 mL of the previous extraction solvent and centrifuged. Supernatants were pooled and taken to dryness. The dry residue was taken in water and purified on an anion exchanger column (QAE Sephadex A-25, length = 75 cm, diameter = 5 cm; Pharmacia) previously activated in 0.5 M sodium formate, eluted with water (3 mL/min). Fractions containing GHB and GDHB were pooled separately and taken to dryness. Each partial purified extract was applied on a cation exchanger column (SP Sephadex C-25, length = 30 cm, diameter = 3 cm; Pharmacia) activated in 0.5 M ammonium sulfate and eluted with 0.01 M NaCl (3 mL/min). After concentration, the aqueous solutions containing the $\gamma$-glutaminyl derivative were desalted on a QAE Sephadex A-25 column (length = 30 cm, diameter = 2 cm). The GDHB solution was concentrated and stored in fraction aliquots at −20 °C until further analysis. Traces of GDHB present in the GHB extract were removed by adding sodium *m*-periodate ($NaIO_4$) to a final concentration of 1 mM. *o*-Quinones instantaneously formed after *o*-diphenol oxidation were separated from the pure GHB on an SP Sephadex C-25 column (length = 30 cm, diameter = 3 cm) eluted with water (3 mL/min), and GHB was finally crystallized in water.

**GHB/GDHB Analysis.** Chromatographical fractionations were followed spectrophotometrically in a range of 200−400 nm with an ultraviolet−visible Perkin-Elmer Lambda-2 spectrophotometer (Überlingen, Germany) on-line interfaced to a Pentium-100 microcomputer (Ede, The Netherlands). Each step of the purification was followed by thin-layer chromatography on silica gel 60 F254 (Merck) with 60% (v/v) butanol in 15% (v/v) acetic acid as mobile phase (Datta and Hoesch, 1987) and reversed phase HPLC column (Hypersil BDS C18, 5 $\mu$m, 250 × 4.6 mm, Alltech, Deerfield, IL) using as mobile phase 1.8% (v/v) trifluoroacetic acid (solvent A) and 10% (v/v) acetonitrile in 1.8% (v/v) trifluoroacetic acid (solvent B) following a gradient (0−20 min, 5−46% B) at a flow rate of 1 mL/min. Detection was performed by monitoring absorbance at 224 and 245 nm with a UV detector (Pharmacia).

**Spectrophotometric Assays.** Kinetic assays were carried out by measuring the appearance of the product in the reaction medium in the above-described spectrophotometer. Temperature was controlled at 25 °C with a circulating bath with a heater/cooler and checked using a precision of ±0.1 °C. The reference cuvette contained all of the components except the substrate with a final volume of 1 mL.

Monophenolase activity of tyrosinase on GHB and L-Tyr and diphenolase activity of tyrosinase on GDHB and L-DOPA were determined spectrophotometrically by using MBTH, which is a potent nucleophile through its amino group, which realizes the nucleophilic attack on the *o*-quinones (Espín et al., 1995a, 1996, 1997a, 1998a). This assay method is highly sensitive, reliable, and precise. MBTH traps the enzyme-generated *o*-quinones, rendering MBTH−quinone adducts with high molar extinction coefficients.

**Oxymetric Assays.** Oxygen consumption was followed with a YSI Model 5300 oxymeter (Yellow Springs, OH) based on the Clark electrode with a Teflon membrane equipped with a Kipp & Zonen recorder (Breukelen, The Netherlands). Calibration was made by using the 4-*tert*-butylcatechol/tyrosinase method (Rodríguez-López et al., 1992b).

**NMR Assays.** $^{13}C$ NMR spectra of the phenolic compounds assayed were obtained with an AMX-400 MHz spectrometer. The spectra were measured at pH 6.8 using $D_2O$ as solvent. $\delta_3$ and $\delta_4$ for *o*-diphenols and $\delta_4$ for monophenols were measured relative to those for tetramethylsilane ($\delta = 0$). The maximum line width accepted in the NMR spectra was 0.06 Hz.

**Kinetic Data Analysis.** The values of $K_m$ and $V_{max}$ for the monophenols (GHB and L-tyrosine) and *o*-diphenols (GDHB and L-DOPA) were calculated from triplicate measurements of the steady-state rate, $V_{ss}$, for each initial substrate concentration ($[S]_0$). The reciprocals of the variances of $V_{ss}$ were used as weight factors to the nonlinear regression fitting of $V_{ss}$ versus $[S]_0$ to the Michaelis equation (Wilkinson, 1961; Endrenyi, 1981). The fitting was carried out by using a Gauss−Newton algorithm (Marquardt, 1963) implemented in the Sigma Plot 2.01 program for Windows (Jandel Scientific, 1994).

The values of $V_{max}^{O_2}$ and $K_m^{O_2}$ on oxygen of tyrosinase using the different phenolic compounds were calculated from the curvature in 10 plots of the oxygen consumption versus time (Rodríguez-López et al., 1993). In these experiments, saturating monophenol or *o*-diphenol concentrations were used. In the monophenolase activity, a certain amount of the corresponding *o*-diphenol was added to ascertain that the system started in the steady state, without any lag period (Espín et al., 1995b, 1997a−f, 1998d). These data were fitted by nonlinear regression to the integrated form of the Michaelis equation using the computer program DNRPEASY (Duggleby, 1984).

**Other Methods.** Protein content was determined by using the method of Bradford (1976) using bovine serum albumin as standard.

## RESULTS AND DISCUSSION

**Formation and Properties of the MBTH−Quinone Adducts.** One of the most important problems that has to be solved in the characterization of tyrosinase activity is the instability of the reaction products. This problem is especially remarkable in the monophenolase activity of tyrosinase, which usually requires long assay times. The enzyme-generated *o*-quinones are very unstable and evolve nonenzymatically to render melanins. In the case of L-tyrosine and L-DOPA this problem was solved by measuring at 484 nm the appearance of the corresponding MBTH−quinone adduct (Espín et al., 1997a, 1998c,d).

A tentative model for the oxidation of GHB and GDHB catalyzed by tyrosinase in the presence of MBTH is proposed (Scheme 1). This reaction mechanism is based on those previously proposed for other monophenols (Espín et al., 1995a,b, 1996, 1997a−f, 1998a−d). The main species (MBTH−quinone adduct) accumulated in the assay was the protonated *p*-quinoid structure $AH^+$ (AH1 and AH2 in a tautomery shifted toward the *p*-quinoid structure AH2. This species (AH2), reddish in color, is the main species detected as described by the thick arrows in Scheme 1. The deprotonation of these species to render the oxidizable product (A) is very slow, and therefore the accumulation of the final *o*-quinoid adduct (B) is also very slow (Scheme 1; Espín et al., 1997a).

A high tyrosinase concentration catalyzed the oxidation of low GDHB concentrations in the presence of MBTH to render the MBTH−quinone adduct (Figure 1A). The formation of the MBTH−quinone adduct was carried out at several pH values (Table 1). At low pH the adduct was soluble and stable (Figure 1A, dashed

**Scheme 1. Sequence of Reactions for the Monophenolase and Diphenolase Activities of Tyrosinase on GHB and GDHB in the Presence of MBTH[a]**

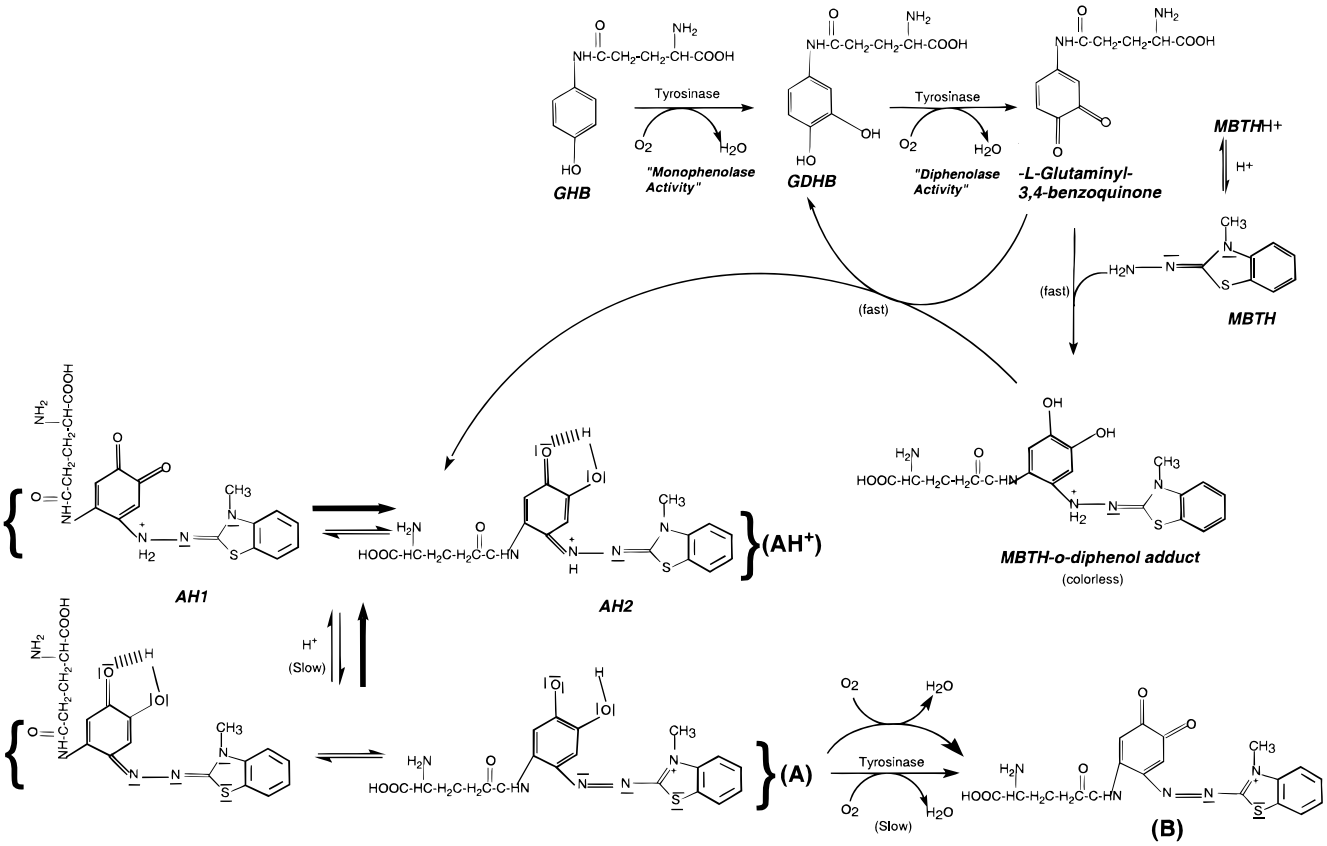


[a] $AH^+$, protonated *p*-quinoid adduct (tautomery between AH1 and AH2 in an equilibrium shifted toward AH2); A, deprotonated *p*-quinoid adduct; B, oxidized MBTH−*o*-quinone adduct after $AH^+$ evolution (Espín et al., 1997b). Reactions for monophenolase and diphenolase activities of tyrosinase are detailed in Scheme 2. When the side chain is $CH_2-CHNH_2-COOH$, the substrate is tyrosine or DOPA.

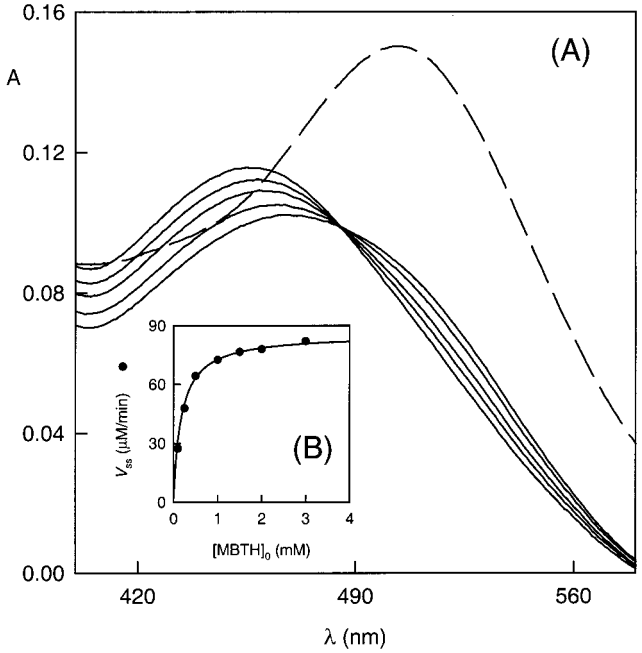


**Figure 1.** (A) Scan spectra for the oxidation of GDHB catalyzed by mushroom tyrosinase in the presence of MBTH. Conditions were as follows: 5 $\mu$M GDHB, 2% DMF, 0.2 mM MBTH, 0.3 $\mu$g/mL mushroom tyrosinase, and 50 mM AB (pH 4.5) (dashed line) or 50 mM PB (pH 6.8) (solid lines). Time between recordings was 300 s. (B) Determination of the saturating MBTH concentration in the oxidation of GDHB catalyzed by mushroom tyrosinase. Conditions were as follows: 5 mM GDHB, 2% DMF, 50 mM PB (pH 6.8), and 0.09 $\mu$g/mL tyrosinase.

**Table 1. $[MBTH]_{sat}$, Visible $\lambda_{max}$, $\lambda_i$, and Molar Extinction Coefficients for the MBTH−Quinone Adduct of GHB and GDHB as a Function of pH[a]**

| pH | $[MBTH]_{sat}$ (mM) | $\lambda_{max}$ (nm) | $\lambda_i$ (nm) | $\epsilon_{max}$ ($M^{-1}$ $cm^{-1}$) | $\epsilon_i$ ($M^{-1}$ $cm^{-1}$) |
|---|---|---|---|---|---|
| 4.5 | 0.20 ± 0.01 | 503 | | 30000 ± 800 | |
| 5.5 | 0.45 ± 0.03 | 503 | 497 | | 28500 ± 800 |
| 6.0 | 1.05 ± 0.07 | 503 | 486 | | 26500 ± 700 |
| 6.5 | 2.30 ± 0.10 | 503 | 486 | | 24000 ± 600 |
| 6.8 | 3.00 ± 0.15 | 503 | 484 | | 19000 ± 400 |
| 7.0 | 3.15 ± 0.15 | 503 | 484 | | 19000 ± 400 |
| 7.3 | 3.50 ± 0.22 | 503 | 481 | | 17000 ± 300 |

[a] Conditions were as follows: 50 mM AB (pH 4.5−5.5), 50 mM PB (pH 6−7.3), 5 $\mu$M GDHB, 2% DMF, the range of MBTH varied from $[MBTH]_{sat}/10$ to 2 $[MBTH]_{sat}$, and 0.3 $\mu$g/mL mushroom tyrosinase.

line), but at higher pH it was soluble and evolved showing an isosbestic point (Figure 1A, solid lines) (Espín et al., 1995a, 1996, 1997a, 1998a). The saturating MBTH concentration ($[MBHT]_{sat}$) to trap all of the enzymatically generated *o*-quinone was determined by measuring the initial rate of change in absorbance at the maximum or isosbestic wavelength of the adduct, using different amounts of MBTH (Figure 1B; Table 1). The oxidation of GHB and GDHB gave rise to an unstable *o*-quinone ($\gamma$-L-3,4-benzoquinone) (Figure 2A) with low molar extinction coefficient, which made the measurement of its accumulation unreliable. This *o*-quinone evolved through first-order kinetics to render the "490" product (iminoquinone, which also appeared following first-order kinetics) (Figure 2A), which was not stable (Jolivet et al., 1998). The determination of these

**Table 2. Kinetic Constants for the Monophenolase and Diphenolase Activities of Mushroom Tyrosinase on Some Physiological Substrates**[a]

| substrate | $V_{max}$ ($\mu$M/min) | $K_m$ (mM) | $V_{max}^{O_2}$ ($\mu$M/min) | $K_m^{O_2}$ ($\mu$M) | $V_{max}/K_m$ ($min^{-1}$) | $V_{max}^{O_2}/K_m^{O_2}$ ($min^{-1}$) |
|---|---|---|---|---|---|---|
| GHB | 2.10 ± 0.10 | 0.30 ± 0.03 | 3.20 ± 0.21 | 1.50 ± 0.12 | $6.7 \times 10^{-3} \pm 9.8 \times 10^{-4}$ | 2.13 ± 0.31 |
| GDHB | 210.10 ± 7.30 | 7.80 ± 0.41 | 200.20 ± 8.10 | 100.20 ± 8.22 | $2.7 \times 10^{-2} \pm 2.1 \times 10^{-3}$ | 2.00 ± 0.24 |
| L-Tyr | 3.10 ± 0.15 | 0.50 ± 0.04 | 4.70 ± 0.21 | 2.10 ± 0.11 | $6.2 \times 10^{-3} \pm 7.9 \times 10^{-4}$ | 2.24 ± 0.22 |
| L-DOPA | 91.60 ± 4.20 | 1.50 ± 0.07 | 90.40 ± 5.00 | 38.20 ± 3.10 | $8.9 \times 10^{-2} \pm 8.3 \times 10^{-3}$ | 2.36 ± 0.31 |

[a] Conditions were as follows: 50 mM PB (pH 6.8), 2% DMF, $[MBTH]_{sat}$, and different substrate concentrations. $V_{max}$ and $V_{max}^{O_2}$ are related to 0.03 $\mu$g/mL mushroom tyrosinase.

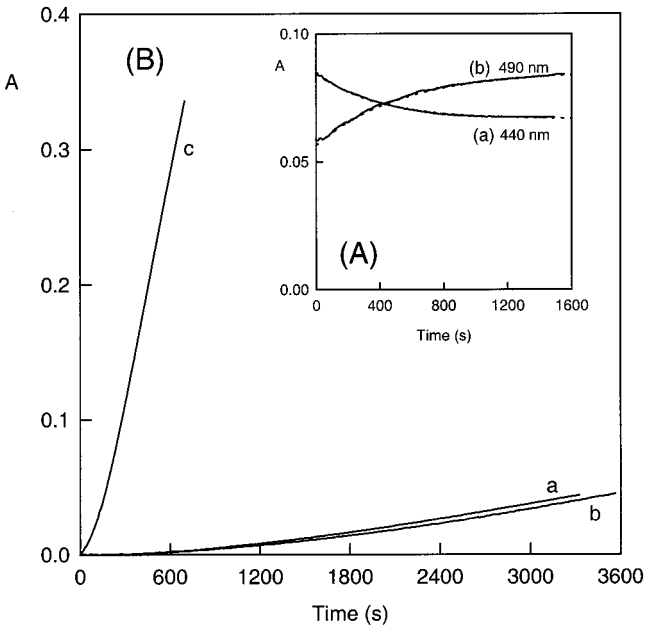


**Figure 2.** (A) Spectrophotometric recording of the monophenolase activity of mushroom tyrosinase. Conditions were as follows: 50 mM PB (pH 6.8), 0.5 mM GHB, 0.09 $\mu$g/mL tyrosinase; (a) GHB alone, at 440 nm; (b) GHB alone, at 490 nm; (c) GHB with 3 mM MBTH and 2% DMF, at 484 nm. (B) Spectrophotometric recording of the formation of $\gamma$-L-3,4-benzoquinone (curve a, 440 nm) and iminoquinone (curve b, 490 nm). Conditions were as follows: 65 $\mu$M GDHB, 50 mM PB (pH 6.8), and 0.1 mM $NaIO_4$. Recording a was fitted to a decreasing uniexponential equation with an apparent evolution constant ($\lambda$) of $2.4 \times 10^{-3}$ $s^{-1}$. Recording b was fitted to an increasing uniexponential equation with an apparent evolution constant ($\lambda$) of $2.2 \times 10^{-3}$ $s^{-1}$.

reaction products required very long assay times and, moreover, the system could not reach the steady state because of the instability of the products (Figure 2B). It is important to note that in the same assay both products, $\gamma$-L-3,4-benzoquinone and iminoquinone, were accumulated at the same time as a consequence of the instability of $\gamma$-L-3,4-benzoquinone (Figure 2A,B, curves a and b). However, in the presence of MBTH, the monophenolase activity of tyrosinase on GHB reached the steady state in short assay time with high sensitivity (Figure 2A, curve c).

**Reaction Mechanism of Tyrosinase.** The melanogenesis pathway from monophenol starts with the monophenolase activity of tyrosinase, which consists of two catalytic cycles overlapping through three common forms of the enzyme *met*tyrosinase ($E_m$), *oxy*tyrosinase ($E_o$), and *deoxy*tyrosinase ($E_d$) (Schoot-Uiterkamp et al., 1976; Rodríguez-López et al., 1992b; Solomon et al., 1996; Espín et al., 1998d) (Scheme 2). The reaction mechanism presented here (Scheme 2) combines the three states of the enzyme and binding and catalytic steps in the monophenolase and diphenolase activities of tyrosinase (Rodríguez-López et al., 1992a; Espín et al., 1998d). The stoichiometry of the pathway implies that one molecule of tyrosinase must accomplish two turnovers in the hydroxylase cycle for each one in the oxidase cycle (Rodríguez-López et al., 1992a; Ros et al., 1994a). This stoichiometry predicts that $V_{max}^{O_2}/V_{max} = 1.5$ for the monophenolase activity and $V_{max}^{O_2}/V_{max} = 1$ for the diphenolase activity. These ratios were verified experimentally for the oxidation of GHB, L-Tyr, GDHB, and L-DOPA (Table 2) (Rodríguez-López et al., 1992a; Ros et al., 1994a; Espín et al., 1997b).

The $E_m$ form of the enzyme does not act on monophenols and binds them through a dead-end pathway. The resulting form is a dead-end complex ($E_m$−M) (Rodríguez-López et al., 1992a; Ros et al., 1994a; Sánchez-Ferrer et al., 1995; Espín et al., 1997b, 1998d). The existence of this $E_m$−M complex may explain the existence of a lag period ($\tau$) prior to the steady-state rate ($V_{ss}$). In this steady state the system reaches a constant *o*-diphenol concentration ($[D]_{ss}$). For *o*-diphenol generation and consumption rates to be equal, a certain time is necessary. This time is the lag period, which can be reduced or eliminated by adding small amounts of *o*-diphenol (Rodríguez-López et al., 1992a; Ros et al., 1994a; Espín et al., 1995b, 1997a−f). Several tests, detailed below, can be performed to verify if the oxidation of GHB catalyzed by mushroom tyrosinase fulfilled the reaction mechanism previously proposed for this enzyme (Rodríguez-López et al., 1992a; Ros et al., 1994a; Espín et al., 1997b, 1998d).

**Effect of pH.** The monophenolase activity of tyrosinase on GHB increased as the pH was increased (Figure 3). The pH also affected the lag period (Figure 3). Low pH caused the protonation of the $E_m$ form of the enzyme, which had lower affinity toward monophenol (GHB) and therefore there was less enzyme in the dead-end complex $E_m$−M and less time was required to reach the steady state (Scheme 2) (Rodríguez-López et al., 1992a; Ros et al., 1994a; Espín et al., 1995b, 1997a−f, 1998a,d).

**Effect of Enzyme Concentration.** An increase in tyrosinase concentration ($[E]_0$) caused a decrease in the lag period ($\tau$) and a linear increase in the steady-state rate ($V_{ss}$) (Figure 4). Increasing $[E]_0$ resulted in an increase in the absolute concentration of $E_o$ form (active on monophenols). Therefore, the formation of *o*-diphenol (GDHB) to reach the steady state was accelerated and $\tau$ diminished (Scheme 2) (Rodríguez-López et al., 1992a; Ros et al., 1994a; Espín et al., 1995b, 1997a−f, 1998a,d).

**Effect of Monophenol ($[GHB]_0$) Concentration.** Both $V_{ss}$ and $\tau$ increased when $[GHB]_0$ was increased (Figure 5). The $E_m$ form of the enzyme was saturated when the $[GHB]_0$ concentration was raised, and there was more enzyme in the dead-end complex $E_m$−M, requiring more time to reach the steady state. Because the system needed more time to reach the steady state, $\tau$ increased (Scheme 2) (Rodríguez-López et al., 1992a; Ros et al., 1994a; Espín et al., 1995b, 1997a−f, 1998a,d).

It has been previously stated that GHB was unique

**Scheme 2. Reaction Mechanism for the Monophenolase and Diphenolase Activities of Tyrosinase**[a]

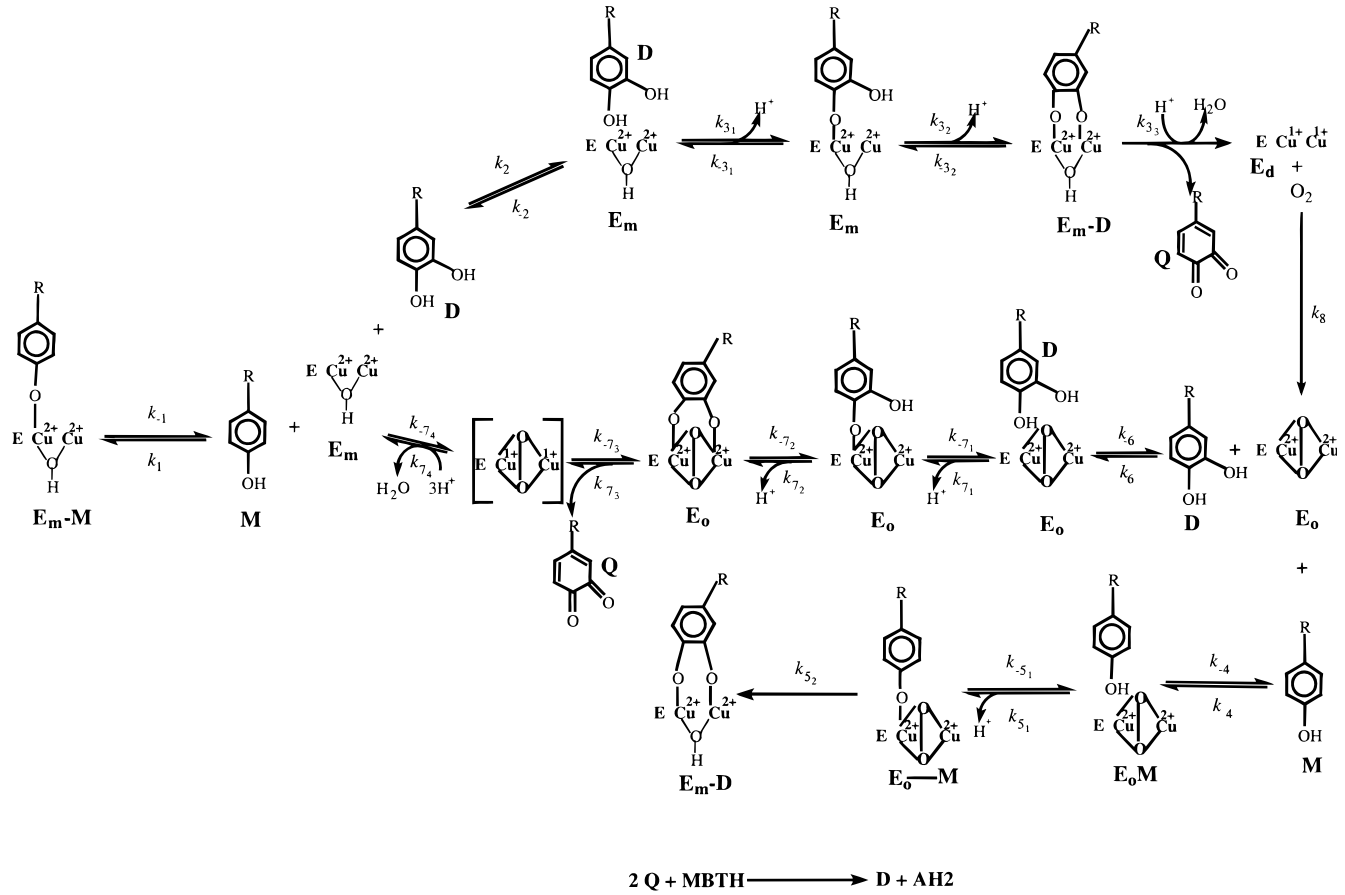


[a] $E_m$, *met*tyrosinase; $E_d$, *deoxy*tyrosinase; $E_o$, *oxy*tyrosinase; M, monophenol (GHB); D, *o*-diphenol (GDHB); Q, *o*-quinone (γ-L-3,4-benzoquinone) (for reaction of Q and MBTH, see Scheme 1); AH2, main MBTH−quinone adduct species detected (see Scheme 1 for details). (The numeric notation of the rate constants is an extension of that previously used in Rodríguez-López et al. (1992) and Espín et al. (1998d).

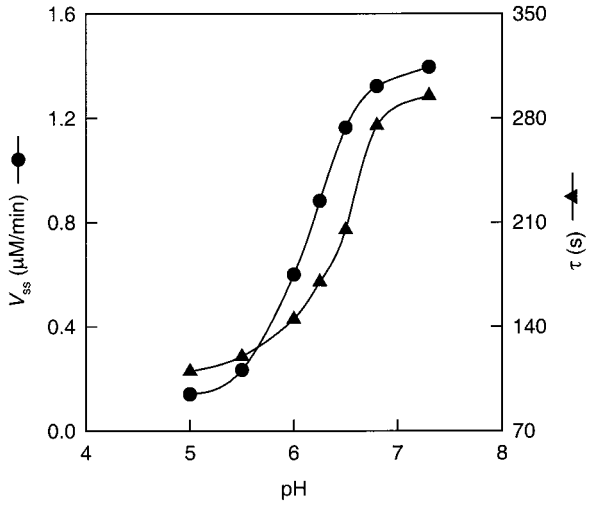


**Figure 3.** Dependence of $\tau$ (▲) and $V_{ss}$ (●) on pH in the oxidation of GHB catalyzed by mushroom tyrosinase in the presence of MBTH. Conditions were as follows: 50 mM AB (pH 5−5.5), 50 mM PB (pH 6−7.3), 2% DMF, saturating MBTH, 0.5 mM GHB, and 0.03 μg/mL tyrosinase.

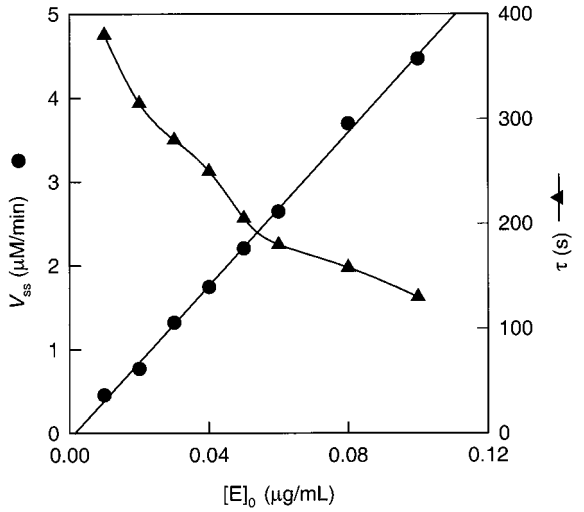


**Figure 4.** Dependence of $\tau$ (▲) and $V_{ss}$ (●) on tyrosinase concentration in the oxidation of GHB catalyzed by tyrosinase in the presence of MBTH. Conditions were as follows: 50 mM PB (pH 6.8), 2% DMF, 3 mM MBTH, and 0.5 mM GHB.

among the monophenolic substrates for tyrosinase because the lag period for the hydroxylation reaction decreased with increasing GHB concentrations (Boekelheide et al., 1979). This must, however, have been an artifact. The presence of *o*-diphenol traces should be taken into account. These traces are very hard to detect by HPLC or other analytical methods but can drastically shorten the lag period. This has been reported for some (synthetic) commercial monophenols such as 4-*tert*-butylphenol (Ros et al., 1994b). The latter monophenol needed further purification (with a column of $Al_2O_3$ activated by ammoniun acetate) to remove *o*-diphenol traces. In the case of the purification from a natural source, the possibility of contamination increases greatly.

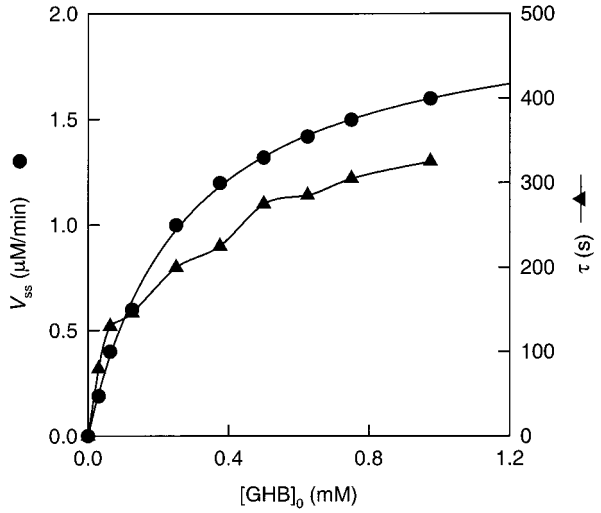


**Figure 5.** Dependence of $\tau$ (▲) and $V_{ss}$ (●) on GHB concentration in the oxidation of GHB catalyzed by tyrosinase in the presence of MBTH. Conditions were as follows: 50 mM PB (pH 6.8), 2% DMF, 3 mM MBTH, and 0.03 $\mu$g/mL tyrosinase. (—) Nonlinear regression fitting of $V_{ss}$ versus [GHB]$_0$.

In our case, the final purification step to remove *o*-diphenol traces was carried out as detailed under Materials and Methods, and it was different from the above previously mentioned (Ros et al., 1994b) because it was not enough to get rid of the *o*-diphenol traces. Without this purification, increasing GHB concentrations (and also increasing GDHB concentrations because of the contamination) decreased the lag period, and at high GHB concentrations even a burst could be observed (see below to explain this phenomenon).

**Effect of *o*-Diphenol ([GDHB]$_0$) Addition.** The addition of different [GDHB]$_0$ to the monophenolase activity diminished $\tau$ (Figure 6A). The system needs to accumulate a certain amount (constant) of *o*-diphenol ([GDHB]$_{ss}$) to reach the steady state. If the initial *o*-diphenol concentration ([GDHB]$_0$) increases, the time required for the steady-state rate level of *o*-diphenol ([GDHB]$_{ss}$) is shortened (Figure 6A). When [GDHB]$_0$ is higher than [GDHB]$_{ss}$, the system must first consume the excess of *o*-diphenol and then gradually consume the monophenol and *o*-diphenol before the steady state rate is finally reached. Under these conditions there was a burst in the activity. Therefore, depending on the assay conditions a negative or positive value for $\tau$ (mathematically expressed) can be observed (Figure 6B) (Scheme 2) (Rodríguez-López et al., 1992a; Ros et al., 1994a; Espín et al., 1995b, 1997a–f, 1998a,d). This can explain the fact that, when there is *o*-diphenol contamination in a monophenol preparation, shorter lag periods and even a burst in the activity can be obtained by adding increasing monophenol concentrations.

**Kinetic and NMR Assays.** $V_{max}$ and $K_m$ values on GHB, GDHB, L-Tyr, and L-DOPA and on oxygen for tyrosinase using the above substrates were determined (Table 2).

To study the influence of the electron donor capacity of the side chain in C-1 toward the benzene ring, the chemical shift values for C-4 ($\delta_4$, in the case of monophenols) and C-3 and C-4 ($\delta_3$ and $\delta_4$, respectively, in the case of *o*-diphenols) were determined by means of NMR assays at the optimum pH of mushroom tyrosinase (Table 3). It has been previously stated that a side chain with a high electron donor capacity (low $\delta$ values) will confer a high nucleophilic power to the oxygen atom

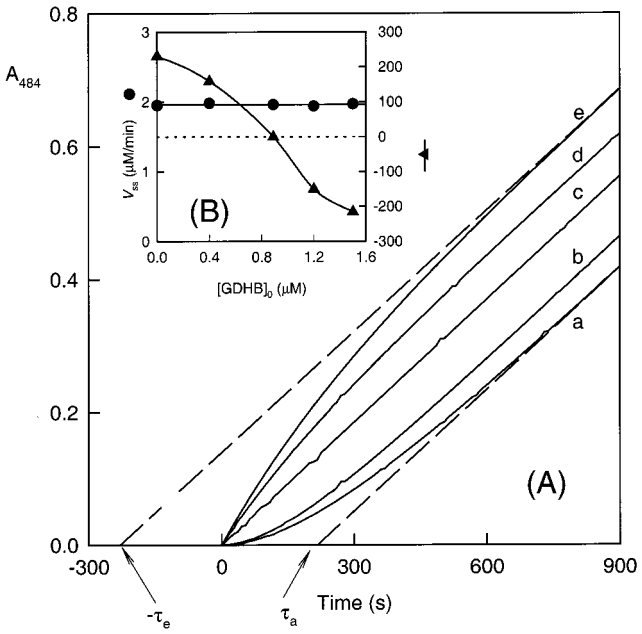


**Figure 6.** (A) Influence of the initial GDHB concentration on the lag period in the oxidation of GHB catalyzed by tyrosinase. Conditions were as follows: 50 mM PB (pH 6.8), 2% DMF, 3 mM MBTH, 0.5 mM GHB, 0.045 $\mu$g/mL tyrosinase, and (a) 0 $\mu$M GDHB, (b) 0.5 $\mu$M GDHB, (c) 0.89 $\mu$M GDHB, (d) 1.2 $\mu$M GDHB, or (e) 1.5 $\mu$M GDHB. (B) Effect of catalytic amounts of GDHB on $\tau$ (▲) and $V_{ss}$ (●). The conditions were the same as detailed above.

**Table 3. $\delta_3$ and $\delta_4$ Values for C-3 and C-4, Respectively, of the Aromatic Ring of Some Phenolic Compounds at pH 6.8[a]**

| substrate | $\delta_3$ | $\delta_4$ | substrate | $\delta_3$ | $\delta_4$ |
|---|---|---|---|---|---|
| GHB | 120.11 | 160.58 | L-Tyr | 118.08[b] | 159.32[b] |
| GDHB | 146.45 | 143.51 | L-DOPA | 146.92[b] | 146.06[b] |

[a] Conditions were as follows: saturating substrate concentration in $D_2O$ at pH 6.8. $\delta$ values were measured relative to those for tetramethylsilane ($\delta = 0$). [b] Espín et al. (1998c).

from the phenolic hydroxyl group (high nucleophilic power) and will facilitate the hydroxylation and oxidation of monophenols and *o*-diphenols, respectively (Espín et al., 1998a–d).

The sequence of the NMR values was $\delta_4^{GHB} > \delta_4^{L-Tyr}$ for C-4 in both monophenols and $\delta_3^{L-DOPA} > \delta_3^{GDHB}$ for C-3 and $\delta_4^{L-DOPA} > \delta_4^{GDHB}$ for C-4 in both *o*-diphenols (Table 3). The velocity of the catalytic action (which was directly related to the $V_{max}$ values) was corroborated by the kinetic $V_{max}$ values of tyrosinase on these compounds (Table 2) (Espín et al., 1998a–d). The sequence obtained for $V_{max}$ values was GDHB > L-DOPA > L-Tyr > GHB, which was in accordance to the order predicted by their respective $\delta$ values (Table 3). However, the sequence of $K_m$ was not in direct relation to their different nucleophilic powers (Espín et al., 1988d).

The oxygen consumption was recorded, and the trace was linear with all of the substrates assayed until around the first 80–90% (depending on the substrate) of oxygen consumption ($r = 0.998$) (results not shown). Therefore, $K_m^{O_2}$ values of tyrosinase on oxygen were very low when the above substrates were used (Table 2). These values were lower for the monophenols GHB and L-Tyr than for the *o*-diphenols GDHB and L-DOPA, which agrees with previous studies on the determination of the oxygen Michaelis constants for tyrosinase (Rodríguez-López et al., 1992b, 1993). The $K_m^{O_2}$ values

reported here for L-Tyr and L-DOPA are different from those previously reported in the literature. Previous works reported also different $K_m^{O_2}$ values for L-DOPA (1.8 and 9.5 $\mu$M; Rodríguez-López et al., 1992b, 1993, respectively). This could be explained by the use of different lots of commercial mushroom tyrosinases, which can differ in their tyrosinase isoform content (Kumar and Flurkey, 1991).

The low $K_m^{O_2}$ values for tyrosinase in the presence of these phenolic compounds indicate that molecular oxygen is unlikely to be limiting in the reaction of tyrosinase because even with traces of oxygen (20−30 $\mu$M) the enzyme catalyzes the oxidation of these substrates with the same rate as in saturating oxygen concentrations. Only the oxygen Michaelis constant for tyrosinase in the presence of GDHB was relatively high (100 $\mu$M). The catalytic power ($V_{max}/K_m$) of tyrosinase toward oxygen in the presence of the different substrates assayed was approximately the same (Table 3).

The catalytic power of tyrosinase on these substrates (Table 3) was L-DOPA > GDHB > GHB ≈ L-Tyr, which was not fully in accordance to the sequence for the $V_{max}$ values because of the relatively high $K_m$ value for GDHB. This could be explained by the effect of the bulky substituent side chain of GDHB, which is higher than that for L-DOPA. This could decrease the affinity of tyrosinase toward GDHB (Espín et al., 1998a,d) and therefore increase the $K_m$ value. The catalytic power of tyrosinase on GHB was slightly higher than that on L-Tyr. This was due to the lower $K_m$ value of GHB. Again, steric and/or hydrophobic effects could justify the difference in the $K_m$ values between GHB and L-Tyr (Espín et al., 1998a,d).

To sum up, the characteristic melanogenous phenolic compounds of *A. bisporus*, GHB and GDHB, fulfilled the kinetic and structural reaction mechanism previously proposed for mushroom tyrosinase (Figures 3−6; Schemes 1 and 2) (Rodríguez-López et al., 1992a; Ros et al., 1994a; Espín et al., 1995a,b, 1996, 1997a−f, 1998a−d). Mushroom tyrosinase will catalyze the oxidation of both GHB/GDHB and L-Tyr/L-DOPA pairs approximately in the same extent according to the kinetic and NMR values obtained (Tables 2 and 3). However, the relative concentration of each pair in the mushroom as well as other possible factors should be taken into consideration to evaluate which pair is more important to yield the enzymatic browning.

Pierce and Rast (1995) found that GHB-melanins obtained in vitro matched the natural *Agaricus* melanins. Therefore, the authors conclude that mushroom browning might result from the oxidation of GHB. These results were confirmed by Hanotel (1994), who inhibited gill ripening and stopped the browning process after ionization of fresh mushroom slices. The analysis of ionized slices showed a breakdown of GHB synthesis while L-Tyr synthesis was enhanced. Therefore, GHB was crucial for the melanin formation.

This work could shed some light on the melanin biosynthesis pathway that takes place in the commercially important mushrooms of the *Agaricus* genus.

## ABBREVIATIONS USED

AB, sodium acetate buffer; C-3, carbon atom in the 3-position of the benzene ring; C-4, carbon atom in the 4-position of the benzene ring; $\delta_3$, chemical shift value for C-3; $\delta_4$, chemical shift value for C-4; $[D]_{ss}$, *o*-diphenol concentration in the steady state; $D_2O$, deuterium oxide (heavy water); DMF, *N*,*N*′-dimethylformamide; L-DOPA, L-3,4-dihydroxyphenylalanine; $[E]_0$, initial tyrosinase concentration; $E_d$, *deoxy*tyrosinase (reduced form of tyrosinase with $Cu^+-Cu^+$ in the active site); $E_m$, *met*tyrosinase with $Cu^{2+}$-$Cu^{2+}$ in the active site; $E_o$, *oxy*tyrosinase ($E_dO_2$ or $E_mO_2^{2-}$); GHB, $\gamma$-glutaminyl-4-hydroxybenzene; $[GHB]_0$, initial GHB concentration; GDHB, $\gamma$-glutaminyl-3,4-dihydroxybenzene; $[GDHB]_{ss}$, GDHB concentration in the steady state; $[GDHB]_0$, initial GDHB concentration; iminoquinone, 2-hydroxy-4-imino-2,5-cyclohexadienone; $K_m$, Michaelis constant of tyrosinase on phenolic compounds; $K_m^{O_2}$, oxygen Michaelis constant for tyrosinase; $\lambda_{max}$, wavelength at the maximum of absorbance; $\lambda_i$, wavelength at the isosbestic point; M, monophenol; MBTH, 3-methyl-2-benzothiazolinone hydrazone; $[MBTH]_{sat}$, saturating MBTH concentration; NMR, nuclear magnetic resonance; PB, sodium phosphate buffer; S, substrate; SDS−PAGE, electrophoresis in polyacrylamide gel in the presence of sodium dodecyl sulfate; L-Tyr, L-tyrosine (4-hydroxyphenylalanine); $V_{max}$, maximum steady-state rate of tyrosinase on phenolic compounds; $V_{ss}$ steady-state rate; $V_{max}^{O_2}$, maximum steady-state rate of tyrosinase on oxygen.

## LITERATURE CITED


Boekelheide, K.; Grahan, D.; Mize, P. D.; Anderson, W.; Jeffs, P. W. Synthesis of $\gamma$-L-glutaminyl-[3,5-$^3$H]4-hydroxybenzene and the study of reactions catalyzed by the tyrosinase of *Agaricus bisporus*. *J. Biol. Chem.* **1979**, *254*, 12185−12191.

Bradford, M. M. A rapid and sensitive method for the quantification of microgram quantities of proteins utilizing the principle of protein-dye binding. *Anal. Biochem.* **1976**, *210*, 727−735.

Datta, S.; Hoesch, L. Novel synthesis of agaritine, a 4-hydrazinobenzyl-alcohol derivative occurring in *Agaricaceae*. *Helv. Chim. Acta* **1987**, *70*, 1261−1267.

Duggleby, R. G. Regression analysis of nonlinear Arrhenius plots: an empirical model and a computer program. *Comput. Biol. Med.* **1984**, *14*, 447−455.

Endrenyi, L. *Kinetic Data Analysis: Design and Analysis of Enzyme and Pharmacokinetics Experiments*; Plenum: New York, 1981.

Espín, J. C.; Morales, M.; Varón, R.; Tudela, J.; García-Cánovas, F. A continuous spectrophotometric method for determining the monophenolase and diphenolase activities of apple polyphenol oxidase. *Anal. Biochem.* **1995a**, *231*, 237−246.

Espín, J. C.; Morales, M.; Varón, R.; Tudela, J.; García-Cánovas, F. Monophenolase activity of polyphenol oxidase from Verdedoncella apple. *J. Agric. Food Chem.* **1995b**, *43*, 2807−2812.

Espín, J. C.; Morales, M.; Varón, R.; Tudela, J.; García-Cánovas, F. A continuous spectrophotometric method for determining the monophenolase and diphenolase activities of pear polyphenol oxidase. *J. Food Sci.* **1996**, *61*, 1177−1181.

Espín, J. C.; Morales, M.; García-Ruiz, P. A.; Tudela, J.; García-Cánovas, F. Improvement of a continuous spectrophotometric method for determining the monophenolase and diphenolase activities of mushroom polyphenol oxidase. *J. Agric. Food Chem.* **1997a**, *45*, 1084−1090.

Espín, J. C.; Varón, R.; Tudela, J.; García-Cánovas, F. Kinetic study of the oxidation of 4-hydroxyanisole catalyzed by tyrosinase. *Biochem. Mol. Biol. Int.* **1997b**, *41*, 1265−1276.

Espín, J. C.; Morales, M.; Varón, R.; Tudela, J.; García-Cánovas, F. Monophenolase activity of polyphenol oxidase from Blanquilla pear. *Phytochemistry* **1997c**, *44*, 17−22.

Espín, J. C.; Trujano, M. F.; Tudela, J.; García-Cánovas, F. Monophenolase activity of polyphenol oxidase from Haas avocado. *J. Agric. Food Chem.* **1997d**, *45*, 1091−1096.

Espín, J. C.; Ochoa, M.; Tudela, J.; García-Cánovas, F. Monophenolase activity of strawberry polyphenol oxidase. *Phytochemistry* **1997e**, *45*, 667−670.

Espín, J. C.; Tudela, J.; García-Cánovas, F. Monophenolase activity of polyphenol oxidase from artichoke heads (*Cynara scolymus L.*). *Lebensm. Wiss. -Technol.* **1997f**, *30*, 819−825.

Espín, J. C.; Tudela, J.; García-Cánovas, F. 4-Hydroxyanisole: the most suitable monophenolic substrate for determining spectrophotometrically the monophenolase activity of polyphenol oxidase from fruits and vegetables. *Anal. Biochem.* **1998a**, *259*, 118−126.

Espín, J. C.; García-Ruiz, P. A.; Tudela, J.; García-Cánovas, F. Study of the stereospecificity in pear and strawberry polyphenol oxidases. *J. Agric. Food Chem.* **1998b**, *46*, 2469−2473.

Espín, J. C.; García-Ruiz, P. A.; Tudela, J.; García-Cánovas, F. Study of stereospecificity in mushroom tyrosinase. *Biochem. J.* **1998c**, *331*, 547−551.

Espín, J. C.; García-Ruiz, P. A.; Tudela, J.; Varón, R.; García-Cánovas, F. Monophenolase and diphenolase reaction mechanisms of apple and pear polyphenol oxidases. *J. Agric. Food Chem.* **1998d**, *46*, 2968−2975.

Graham, D. G.; Tye, R. W.; Vogel, F. S. Inhibition of DNA polymerase from L1210 murine leukemia by a sulfhydryl reagent from *Agaricus bisporus*. *Cancer Res.* **1977**, *37*, 436−439.

Hammond, J. B. W.; Nichols, D. A. Carbohydrate metabolism in *Agaricus bisporus* (Lange) Sing: changes in soluble carbohydrates during growth of mycelium and sporophore. *J. Gen. Microbiol.* **1976**, *93*, 309−320.

Hanotel, L. Effets de l'ionisation sur le bruissement enzymatique de végétaux frais prédécoupés. Cas de l'endive (*Cichorium intybus* L.) et du champignon de Paris (*Agaricus bisporus* (Lange) Imbach). Ph.D. Thesis, Université de Montpellier, 1994.

Jandel Scientific. *Sigma Plot 2.01 for Windows*; Jandel Scientific: Corte Madera, CA, 1994.

Jolivet, S.; Voiland, A., Pellon, G.; Arpin, N. Main factors involved in the browning of *Agaricus bisporus*. In *Mushroom Science XIV, Science and Cultivation of Edible Fungi*; Elliot, T. J., Ed.; Balkema: Rotterdam, The Netherlands, 1995; Vol. 2, pp 695−702.

Jolivet, S.; Arpin, N.; Wichers, H. J.; Pellon, G. *Agaricus bisporus* browning: a review. *Mycol. Res.* **1998**, *102*, 1459−1483.

Kumar, M.; Flurkey, W. H. Activity, isoenzymes and purity of mushroom tyrosinase in commercial preparations. *Phytochemistry* **1991**, *30*, 3899−3902.

Marquardt, D. An algorithm for least-squares estimation of nonlinear parameters. *J. Soc. Ind. Appl. Math.* **1963**, *11*, 431−441.

Oka, Y.; Tsuji, H.; Ogawa, T.; Sasaoka, K. Quantitative determination of the free amino acids and their derivatives in the common edible mushroom, *Agaricus bisporus*. *J. Nutr. Sci. Vitaminol.* **1981**, *27*, 253−262.

Pierce, J. A.; Rast, D. M. A comparison of native and synthetic mushroom melanins by Fourier transform infrared spectroscopy. *Phytochemistry* **1995**, *39*, 49−55.

Prota, G. Progress in the chemistry of melanin and related metabolites. *Med. Res. Rev.* **1988**, *8*, 525−556.

Rast, D.; Stüssi, H.; Zobrist, P. Self-inhibition of the *Agaricus bisporus* spore by $CO_2$ and/or $\gamma$-glutaminyl-4-hydroxybenzene and $\gamma$-glutaminyl-3,4-benzoquinone: a biochemical analysis. *Physiol. Plant.* **1979**, *46*, 227−234.

Rast, D.; Stüssi, H.; Hegnauer, H.; Nyhlen, L. E. Melanins. *In The Fungal Spores*; Turian, G., Hohl, H. R., Eds.; Academic Press: London, U.K., 1981; pp 501−530.

Rodríguez-López, J. N.; Tudela, J.; Varón, R.; García-Carmona, F.; García-Cánovas, F. Analysis of a kinetic model for melanin biosynthesis pathway. *J. Biol. Chem.* **1992a**, *267*, 3801−3810.

Rodríguez-López, J. N.; Ros, J. R.; Varón, R.; García-Cánovas,F. Calibration of a Clark-type electrode by tyrosinase-catalyzed oxidation of 4-*tert*-butylcatechol. *Anal. Biochem.* **1992b**, *202*, 356−360.

Rodríguez-López, J. N.; Ros, J. R.; Varón, R.; García-Cánovas, F. Oxygen Michaelis constants for tyrosinase. *Biochem. J.* **1993**, *293*, 859−866.

Ros, J. R.; Rodríguez-López, J. N.; García-Cánovas, F. Tyrosinase: kinetic analysis of the transient phase and the steady state. *Biochim. Biophys. Acta* **1994a**, *1204*, 33−42.

Ros, J. R.; Rodríguez-López, J. N.; García-Cánovas, F. Kinetics study of the oxidation of 4-*tert*-butylphenol by tyrosinase. *Eur. J. Biochem.* **1994b**, *222*, 449−452.

Sánchez-Ferrer, A.; Rodríguez-López, J. N.; García-Cánovas, F.; García-Carmona, F. Tyrosinase: A comprehensive review of its mechanism. *Biochim. Biophys. Acta* **1995**, *1247*, 1−11.

Schoot-Uiterkamp, A. J. M.; Evans, L. H.; Jolley, R. L.; Mason, H. S. Absorption and circular dichroism spectra of different forms of mushroom tyrosinase. *Biochim. Biophys. Acta* **1976**, *453*, 200−204.

Solomon, E. I.; Sundaram, U. M.; Machonkin, T. E. Multicopper oxidases and oxygenases. *Chem. Rev.* **1996**, *96*, 2563−2605.

Soulier, L.; Foret, V.; Arpin, N. Occurrence of agaritine and $\gamma$-glutamyl-4-hydroxybenzene (GHB) in the fructifying mycelium of *Agaricus bisporus*. *Mycol. Res.* **1993**, *97*, 529−532.

Stüssi, H.; Rast, D. The biosynthesis and possible function of $\gamma$-glutaminyl-4-hydroxybenzene in *Agaricus bisporus*. *Phytochemistry* **1981**, *20*, 2347−2352.

Vogel, F. S.; McGarry, S. J.; Kemper, L. A. K.; Graham, D. G. Bacteriocidal properties of a class of quinoid compounds related to sporulation in the mushroom, *Agaricus bisporus*. *Am. J. Pathol.* **1974**, *76*, 165−174.

Vogel, F. S.; Kemper, L. A. K.; McGarry, S. J.; Graham, D. G. Cytostatic, cytocidal and potential antitumor properties of a class of quinoid compounds, initiators of the dormant state in the spores of *Agaricus bisporus*. *Am. J. Pathol.* **1975**, *78*, 33−45.

Vogel, F. S.; Kemper, L. A.; Boekelheide, K.; Graham, D. G.; Jeffs, P. W. Intracellular activation of $\gamma$-L-glutaminyl-4-hydroxybenzene by tyrosinase, a mechanism for selective cytotoxicity against melanocarcinoma. *Cancer Res.* **1979**, *39*, 1490−1493.

Weaver, R. F.; Rajagopalan, K. V.; Handler, P.; Rosenthal, D.; Jeffs, P. W. Isolation from the mushroom *Agaricus bisporus* and chemical synthesis of $\gamma$-L-glutaminyl-4-hydroxybenzene. *J. Biol. Chem.* **1971**, *246*, 2010−2014.

Wilkinson, G. N. Statistical estimations in enzyme kinetics. *Biochem. J.* **1961**, *80*, 324−332.

Winder, A. J.; Harris, H. New assays for the tyrosine hydroxylase and dopa oxidase activities of tyrosinase. *Eur. J. Biochem.* **1991**, *198*, 317−326.

Received for review October 19, 1998. Revised manuscript received May 26, 1999. Accepted June 2, 1999. J.C.E. and S.J. are holders of Postdoctoral Grants FAIR/CT97-5004 and FAIR/CT96-5040, respectively, from the European Commission under the framework of the Agriculture, Agro-Industry and Fisheries (FAIR) program.

JF981155H